COLLÈGE DE FRANCE 1530

Cuprates supraconducteurs : où en est-on ?

Pseudogap and Nodal/Antinodal Dichotomy: Cluster-DMFT theoretical viewpoint
* Recent progresses *

Cycle 2010-2011

Séminaire – 14/12/2010

Antoine Georges

Collaborators:




Ecole Polytechnique:

M.Ferrero, P.Cornaglia, L.De Leo

Saclay-IPhT: **O.Parcollet**

Columbia: **E.Gull, A.J.Millis**

Rutgers: **G.Kotliar**

- Europhysics.Lett. 85 (2009) 57009
- Phys Rev B: 80, 064501 (2009); 82, 054502 (2010), 82 ????

Acknowledgements:

- M.Civelli, M.Capone, F.Lechermann, L.de Medici
- A.Sacuto, M.Le Tacon, S.Blanc, W.Guyard, M.Cazayous, Y.Gallais, D.Colson, A.Forget

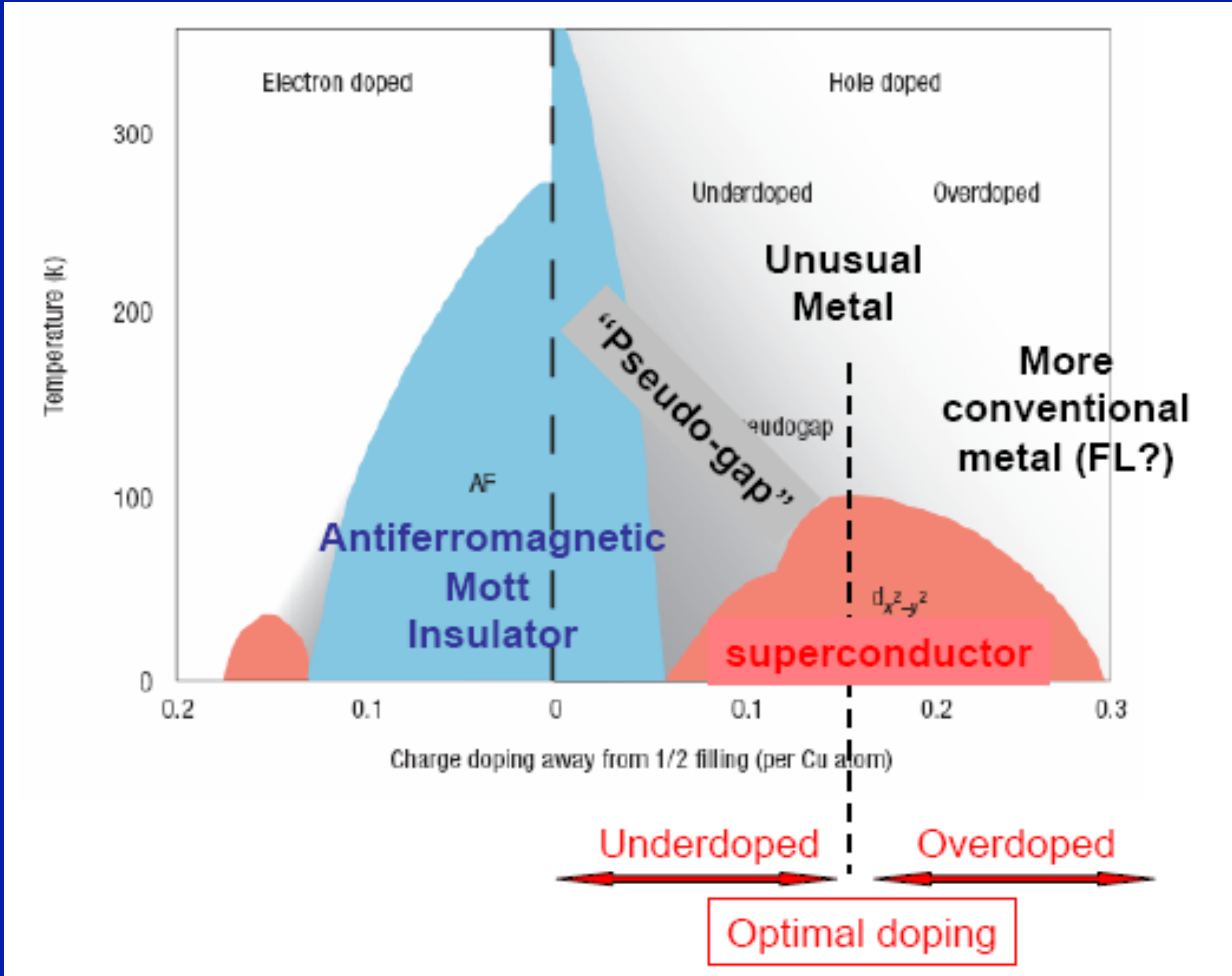

Electron doped
Hole doped
Temperature (K)
300
200
100
0
0.2
0.1
0
0.1
0.2
0.3
Charge doping away from 1/2 filling (per Cu atom)
Underdoped
Overdoped
Unusual Metal
More conventional metal (FL?)
"Pseudo-gap"
AF
Antiferromagnetic Mott Insulator
superconductor
Underdoped
Overdoped
Optimal doping

NORMAL state:

- ``Nodal'' regions display reasonably coherent quasiparticles
- In contrast, excitations in the ``antinodal'' regions e.g. (0,π) are much more incoherent

AND they are (pseudo-) gapped below T*

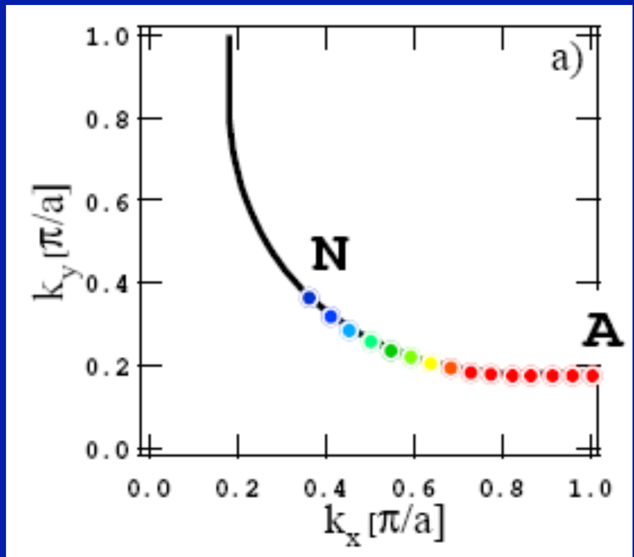

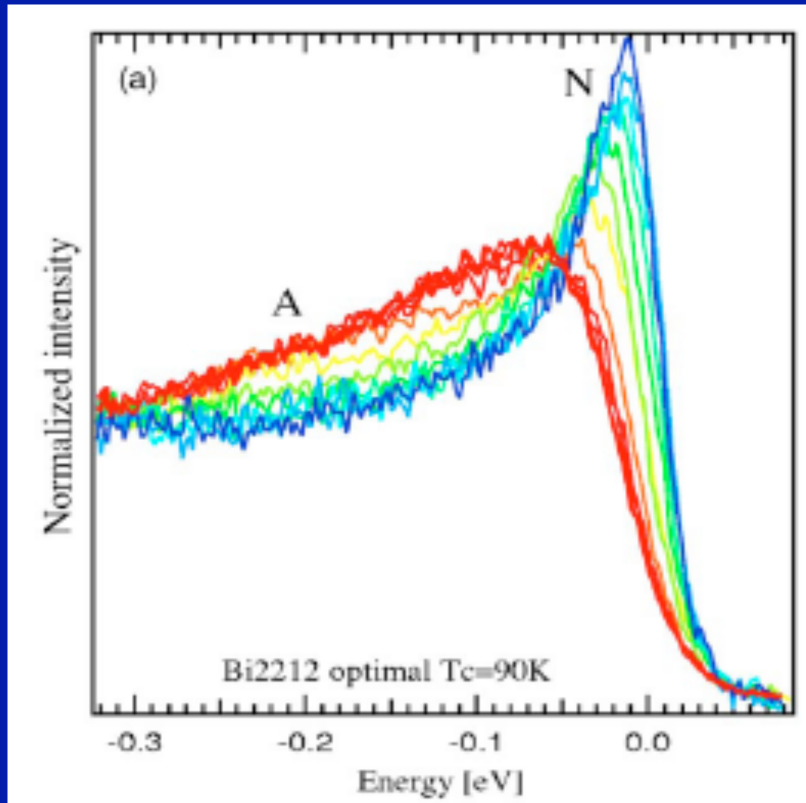

Kaminski et al., 2004 Bi2212
Tc=90K@T=140K

ARPES sees « Fermi arcs »

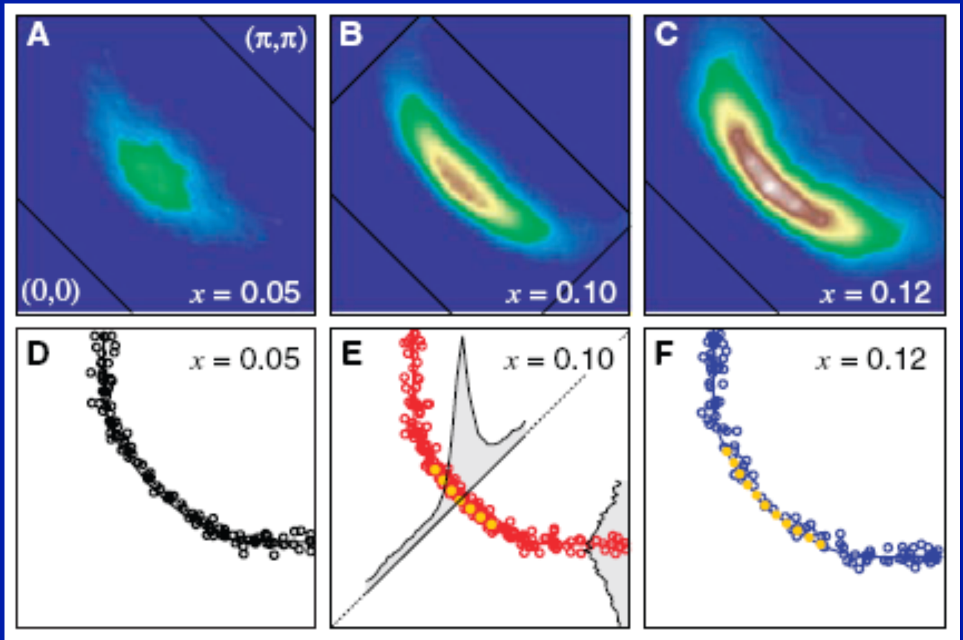

$Ca_{2-x}Na_xCuO_2Cl_2$

K.Shen et al. Science 2007

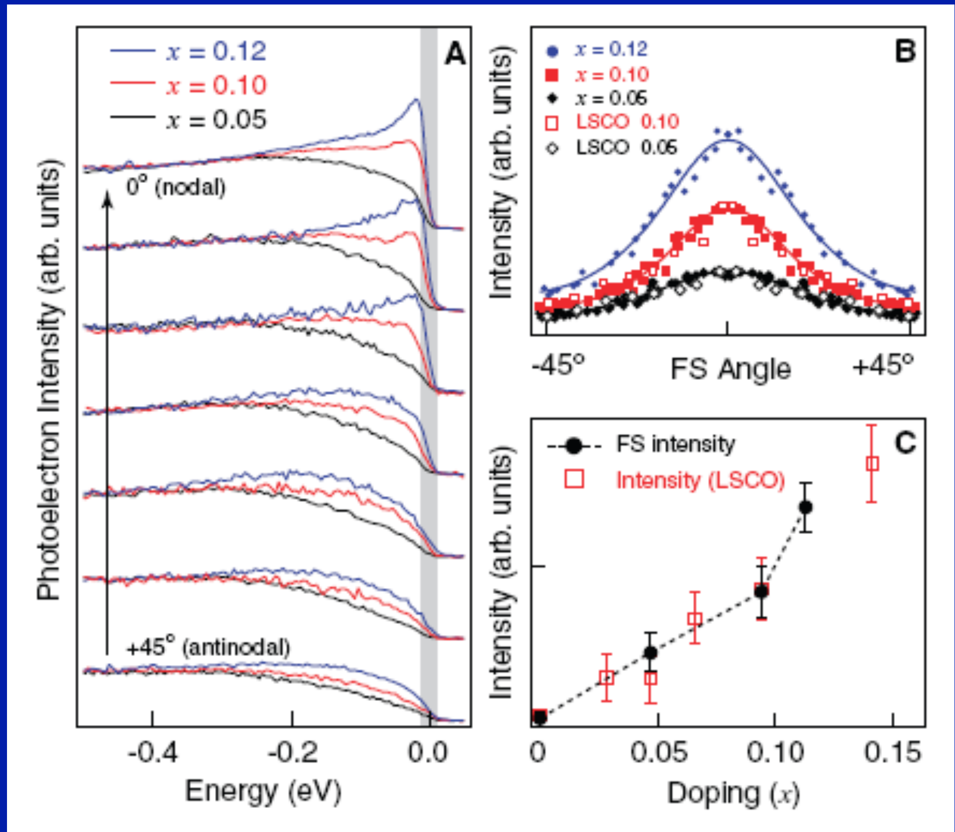

Physical origin of the pseudogap ?

* Fluctuations of the SC order parameter → most probaby NOT
* Long-range ordering ?

cf . seminar by P.Bourges (orbital currents)

→ is it the cause of the PG or a resulting instablity ? [chicken or egg ?]

- Signals formation of singlets due to strong antiferromagnetic superexchange [J] ?

cf. RVB ideas.

Crossover, possibly triggering secondary instability

* Is the PG phenomenon captured by the simplest model: single-band Hubbard or t-J ?

Why is this challenging for theory ?

- Approach to the Mott insulator: *quasiparticle coherence scale*
- Brinkman-Rice/Slave bosons/DMFT: *Uniform scale along Fermi surface* (of order δt)
- Need to take into account inter-site superexchange (J)

→ singlet formation/spatial correlations

Brinkman-Rice/DMFT leads e.g. to a large effective mass ~1/δ
while in fact ~ 1/J is expected for J < δt
(Indeed: spin entropy released at scale J)

From high to low energy/temperature: DMFT and cluster extensions “top to bottom approach”

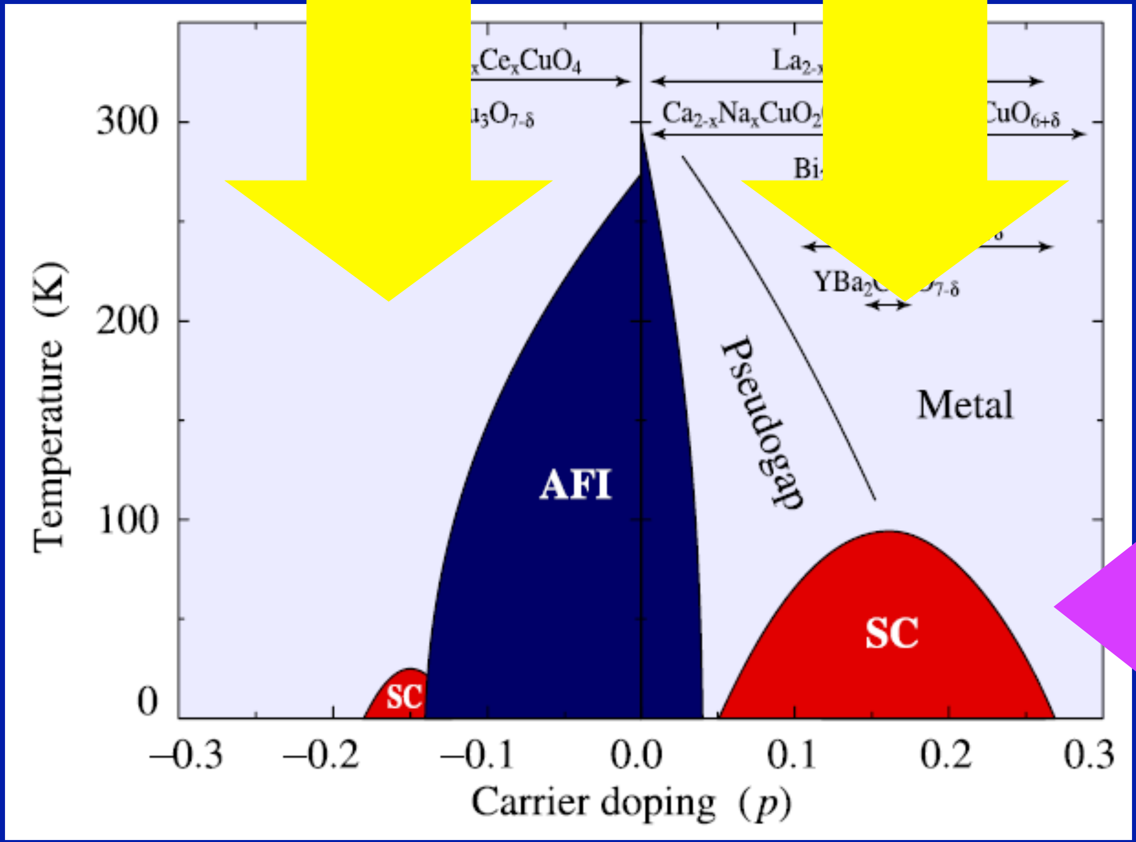

From high to low doping…

Flowing down along RG trajectories…
…Need a « compass » to orient ourselves,

Starting from:

- High-temperature/
- High-energy/
- High-doping level …

At very high doping levels, to the right of the SC dome: physics ~ uniform in momentum space

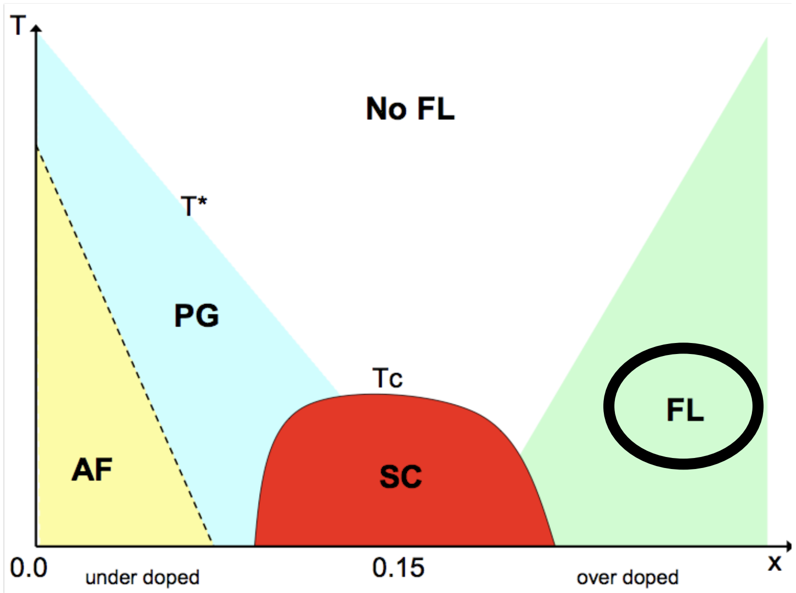

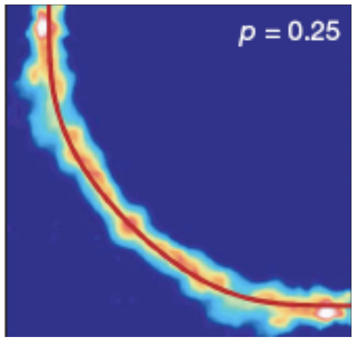

Platé et al., PRL (2005)

Tl2201 OD

Kaminski et al., PRB (2005)

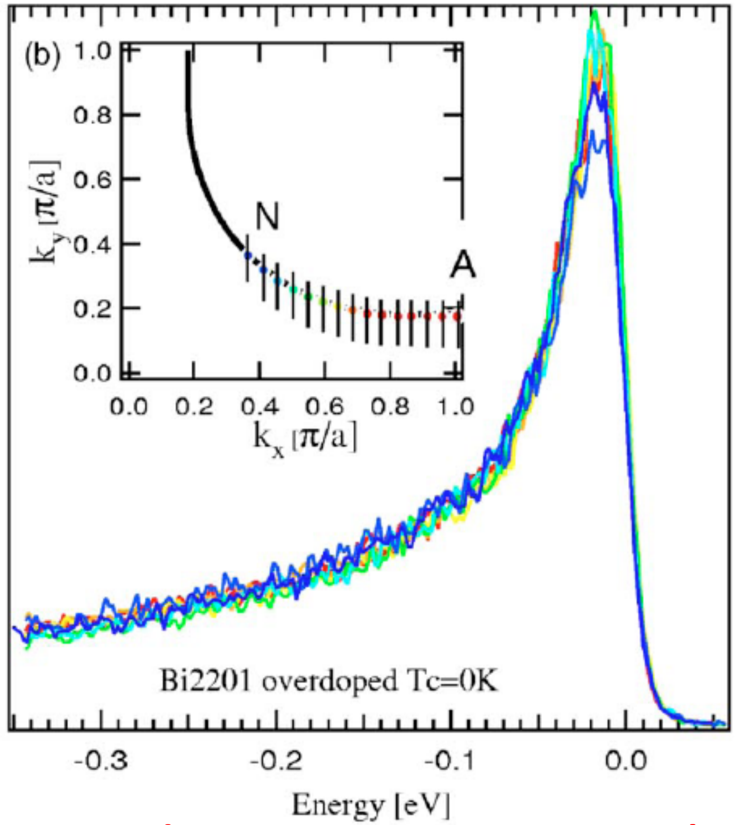

Single-site DMFT is a good approximation in this regime,

Properties are close to that of a Fermi-liquid at low-T, crossover to incoherent at higher T

Dynamical mean-field theory (single-site)

- Provides a simple theory of the proximity of the Mott transition
- Good at describing **the destruction of coherent quasiparticles** (small QP coherence scale, short lifeime near Mott transition)

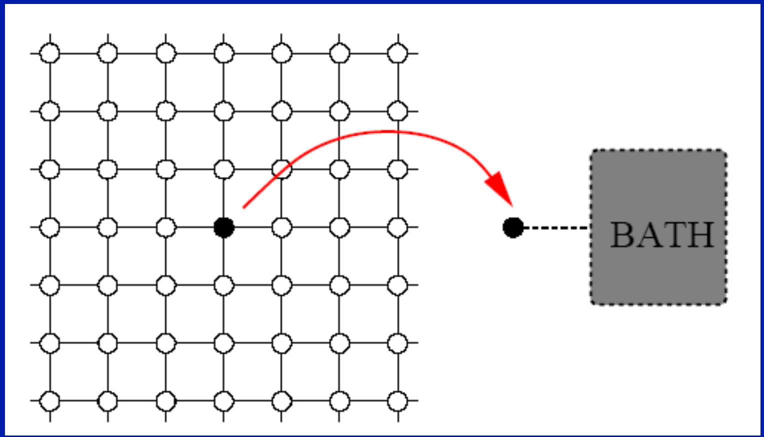

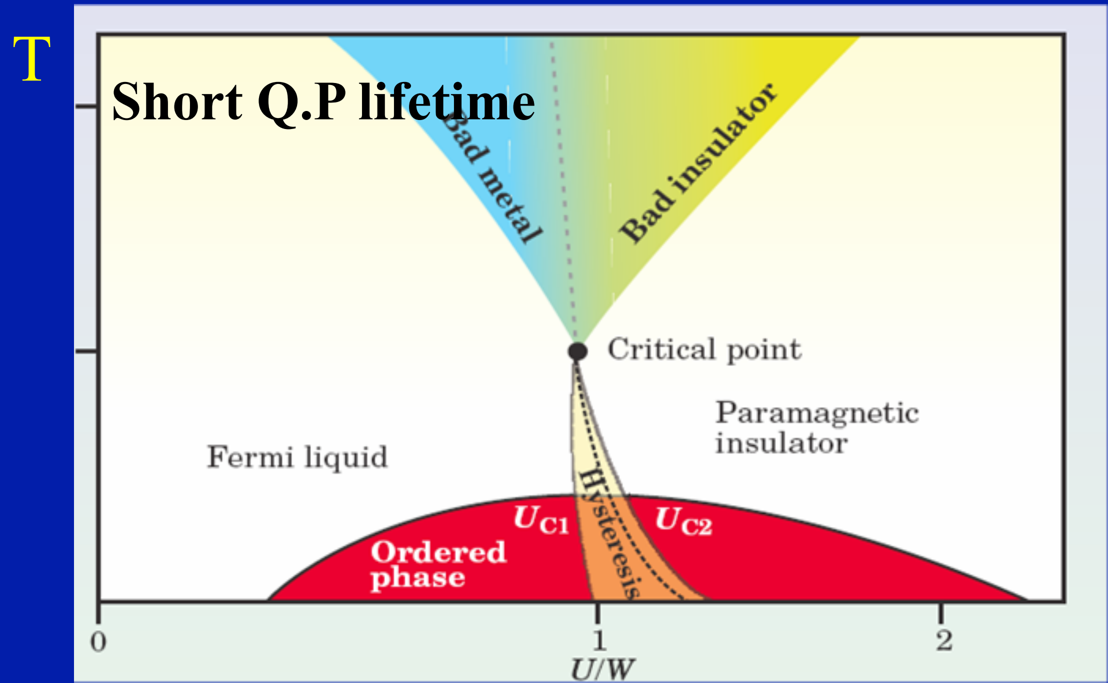

Coherent excitations: k-space (wave)
Incoherent excitations: real space (particle)

2D Hubbard model (t,t',U)

$$H = \sum_{\mathbf{k},\sigma=\uparrow,\downarrow} \varepsilon_{\mathbf{k}} c^{\dagger}_{\sigma\mathbf{k}} c_{\sigma\mathbf{k}} + U \sum_{i} n_{i\downarrow} n_{i\uparrow}$$

$$\varepsilon_{\mathbf{k}} = -2t\left(\cos(\mathbf{k}_x) + \cos(\mathbf{k}_y)\right) - 4t' \cos(\mathbf{k}_x)\cos(\mathbf{k}_y).$$

In the following:

U/t = 10
t'/t = -0.3
Hole-doped
Unit of energy: 4t (= 1)

DMFT equations

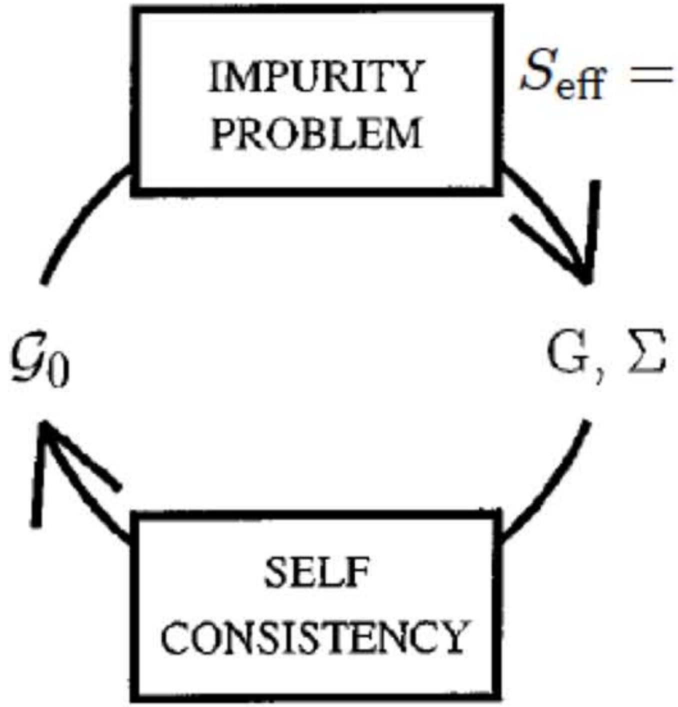

$$S_{\text{eff}} = -\int_0^\beta c_\sigma^\dagger(\tau)\mathcal{G}_0^{-1}(\tau-\tau')c_\sigma(\tau') + \int_0^\beta U n_\uparrow(\tau)n_\downarrow(\tau)$$

$$\Sigma(i\omega_n) = \mathcal{G}_0^{-1}(i\omega_n) - G^{-1}(i\omega_n)$$

$$\Sigma_{\text{lattice}}(i\omega_n, \cancel{k}) \leftarrow \Sigma(i\omega_n)$$

$$G(i\omega_n) = \sum_k G_{\text{lattice}}(i\omega_n, k)$$

$$\mathcal{G}_0^{-1}(i\omega_n) = \left(\sum_k \frac{1}{i\omega_n + \mu - \epsilon_k - \Sigma(i\omega_n)}\right)^{-1} + \Sigma(i\omega_n)$$

In DMFT the self-energy of the lattice is local: Z, m*, coherence temperature, lifetimes are constant along the Fermi surface

Beyond DMFT: accounting for momentum dependence

``Cluster'' extensions - come in various flavors, DCA, CDMFT etc…

For reviews see:

[27] T. Maier, M. Jarrell, T. Pruschke, and M. H. Hettler, Rev. Mod. Phys. 77, 1027 (2005).

[28] G. Kotliar, S. Y. Savrasov, K. Haule, V. S. Oudovenko, O. Parcollet, and C. A. Marianett, Rev. Mod. Phys. 78, 865 (2006).

[29] A. M. S. Tremblay, B. Kyung, and D. Senechal, Low Temp. Phys. 32, 424 (2006).

Previous / Other work on (mostly small) cluster DMFT in 2D:

O. Parcollet, G. Biroli, and G. Kotliar, Phys. Rev. Lett. 92, 226402 (2004), M. Civelli, M. Capone, S. S. Kancharla, O. Parcollet, and G. Kotliar, Phys. Rev. Lett. 95, 106402 (2005), T. Maier, M. Jarrell, T.C. Schulthess, P.R.C. Kent, J.B. White, Phys. Rev. Lett. 95, 237001 (2005), B. Kyung, S. S. Kancharla, D. Sénéchal, A.-M. S. Tremblay, M. Civelli, and G. Kotliar, Phys. Rev. B 73, 165114 (2006), T. D. Stanescu and G. Kotliar, Phys. Rev. B 74, 125110 (2006), A. Macridin, M. Jarrell, T. Maier, P. R. C. Kent, and E. D'Azevedo, Phys. Rev. Lett. 97, 036401 (2006), Y. Z. Zhang and M. Imada, Phys. Rev. B 76, 045108 (2007), M. Civelli, M. Capone, A. Georges, K. Haule, O. Parcollet, T. D. Stanescu, and G. Kotliar, Phys. Rev. Lett. 100, 046402 (2008), E. Gull, P. Werner, X. Wang, M. Troyer, and A. J. Millis, EPL 84, 37009 (2008), H. Park, K. Haule, and G. Kotliar, Phys. Rev. Lett. 101, 186403 (2008), M. Ferrero, P. S. Cornaglia, L. D. Leo, O. Parcollet, G. Kotliar, and A. Georges, EPL 85, 57009 (2009), M. Ferrero, P. S. Cornaglia, L. De Leo, O. Parcollet, G. Kotliar, and A. Georges, Phys. Rev. B 80, 064501 (2009), M. Civelli, Phys. Rev. B 79, 195113 (2009), A. Liebsch and N.-H. Tong, Phys. Rev. B 80, 165126 (2009), N. Lin, E. Gull, and A. J. Millis, Phys. Rev. B 80, 161105(R) (2009), S. Sakai, Y. Motome, and M. Imada, Phys. Rev. Lett. 102, 056404 (2009), G. Sordi, K. Haule, and A. Tremblay, Phys. Rev. Lett. 104, 226402 (2010), S. Sakai, Y. Motome, and M. Imada, arXiv:1004.2569, M. Ferrero, O. Parcollet, G. Kotliar, and A. Georges, arXiv:1001.5051.

Including a k-dependence

Dynamical cluster approximation (DCA)

M. H. Hettler et al., PRB (1998)

T. Maier et al., RMP (2005)

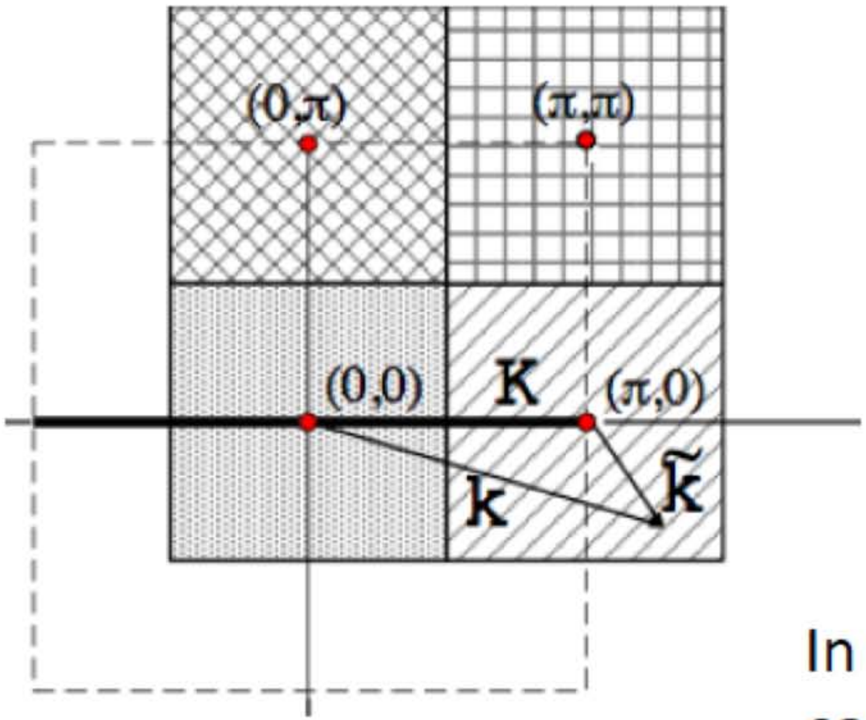

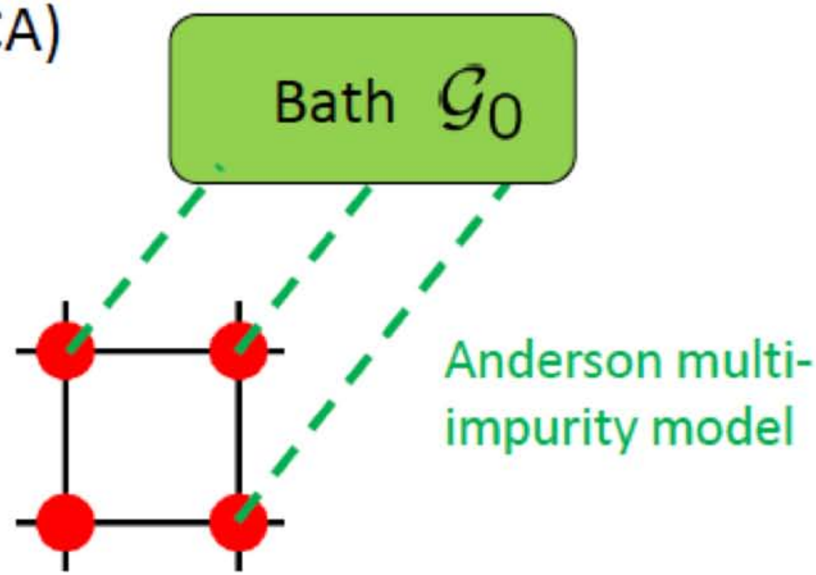

Cluster self-energies for every cluster momenta: $\Sigma(K)$

In DCA, the lattice self-energy is constant over the patches and equal to the cluster self-energies

Two-site DCA: A valence-bond DMFT

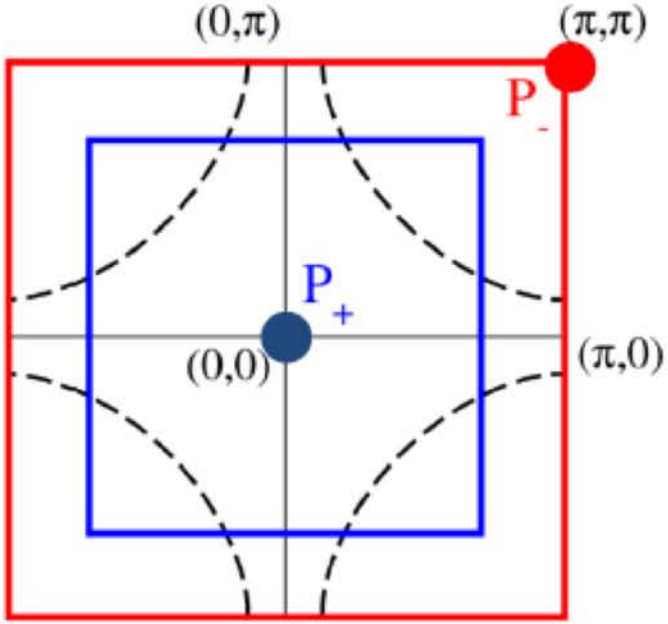

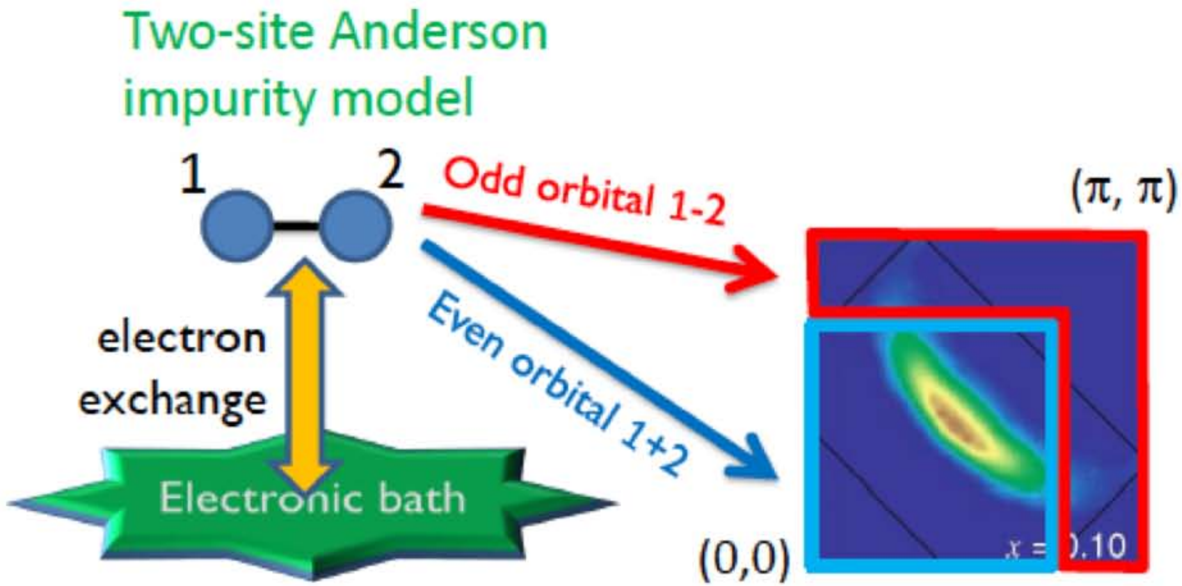

$$\Sigma_{\text{lattice}} = \begin{array}{l} \Sigma_+ \text{ in the central patch} \\ \Sigma_- \text{ in the border patch} \end{array}$$

One patch covers the nodal part of the BZ. The other covers the antinodal part

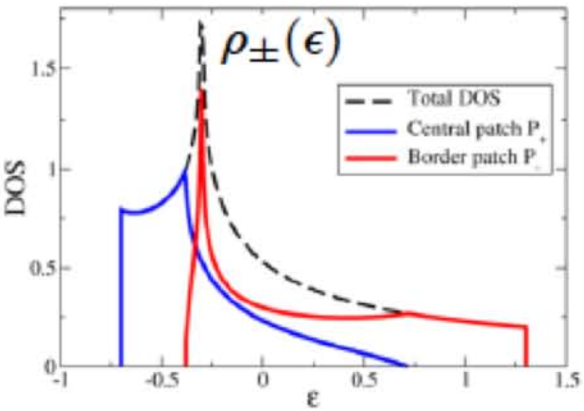

$$\boxed{G_\pm(i\omega_n) = \int \frac{\rho_\pm(\epsilon)}{i\omega_n + \mu - \epsilon - \Sigma_\pm(i\omega_n)}}$$

Solved by CTQMC + Padé approximants

Recent breakthroughs

entering a new age for such approaches…

Continuous-time quantum Monte Carlo (CT-QMC)

***Rubtsov 2005 Interaction expansion(CT-INT)**

***Werner/AJM 2006 Hybridization expansion(CT-HYB)**

***Gull/Parcollet 2008 Auxiliary field (CT-AUX)**

*** Gull 2010 submatrix updates: convergence in cluster size reached for some parameter regime ! (full k-dependence resolved)**

Early studies indicate that DCA/CDMFT schemes can capture pseudogap formation and nodal/antinodal differentiation

PG: Huscroft et al., PRL 2001, N/AN: Civelli et al. PRL 2005

Antinodal Region

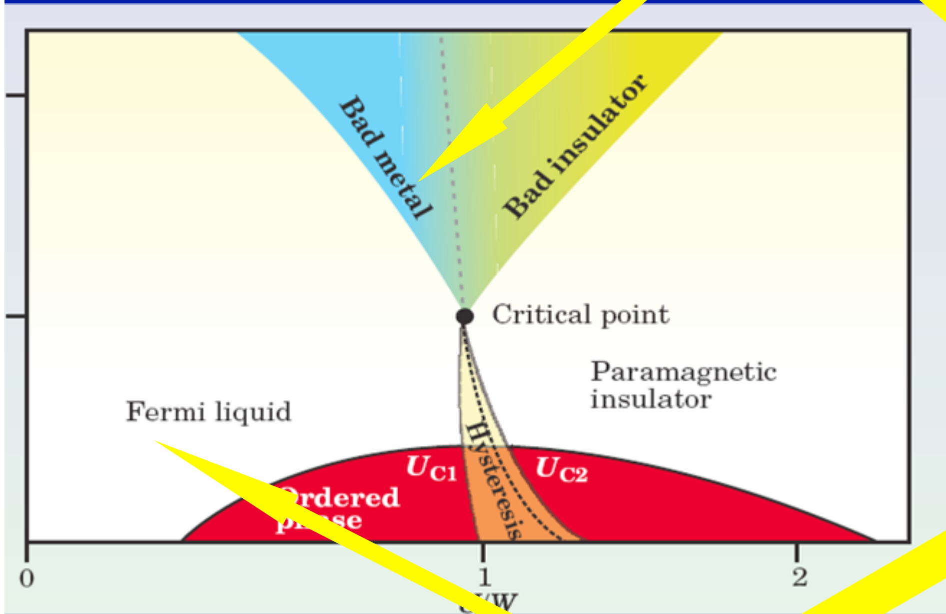

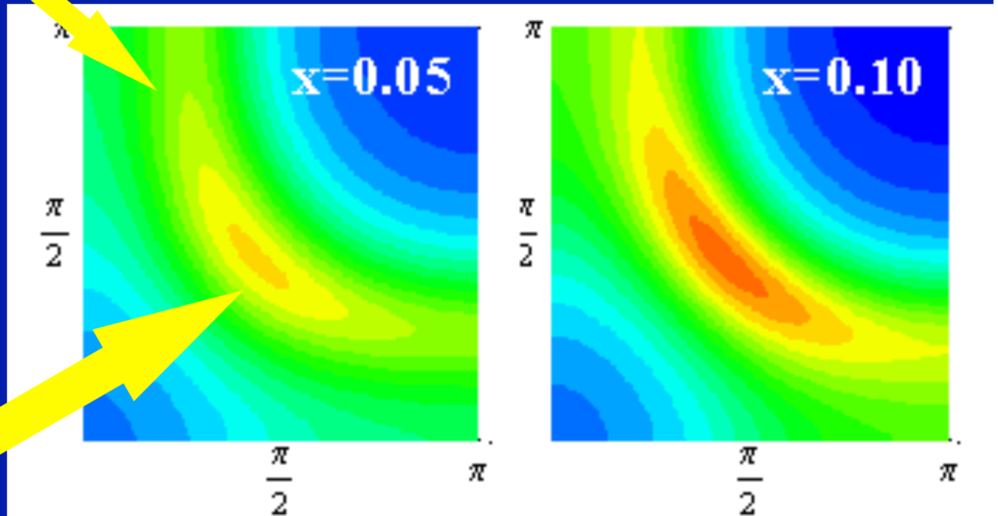

Region near $(\pi,0)$ has higher scattering

Civelli et al., PRL 2005

Nodal Region

How does this work ?

-Physical understanding as a momentum-selective Mott transition

- Generic features
- Systematic studies…

from smallest to huge clusters !

Increasing k-space resolution…

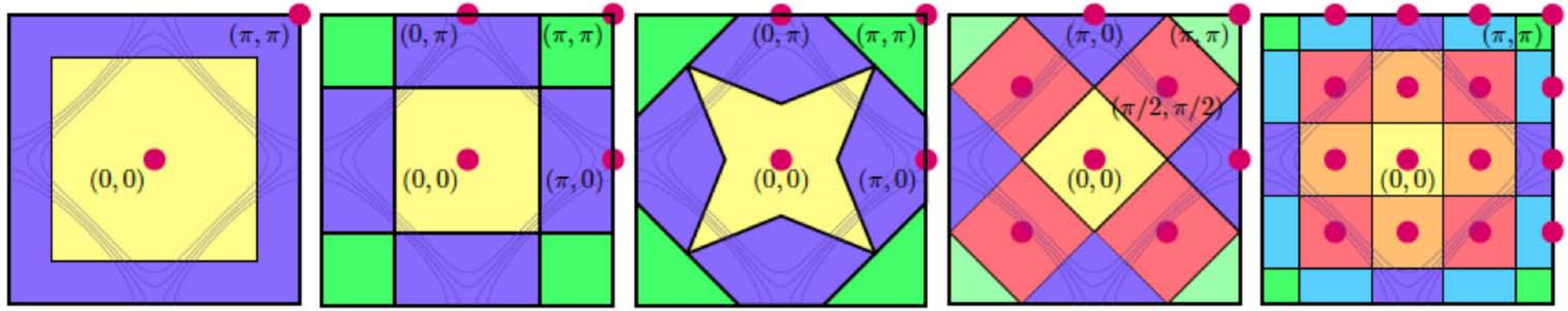

[2,2] [4,4] [4,4]* [5,8] [9,16]

[Patches in ¼ BZ, Sites in real-space cluster]

Generic behavior in different doping regimes

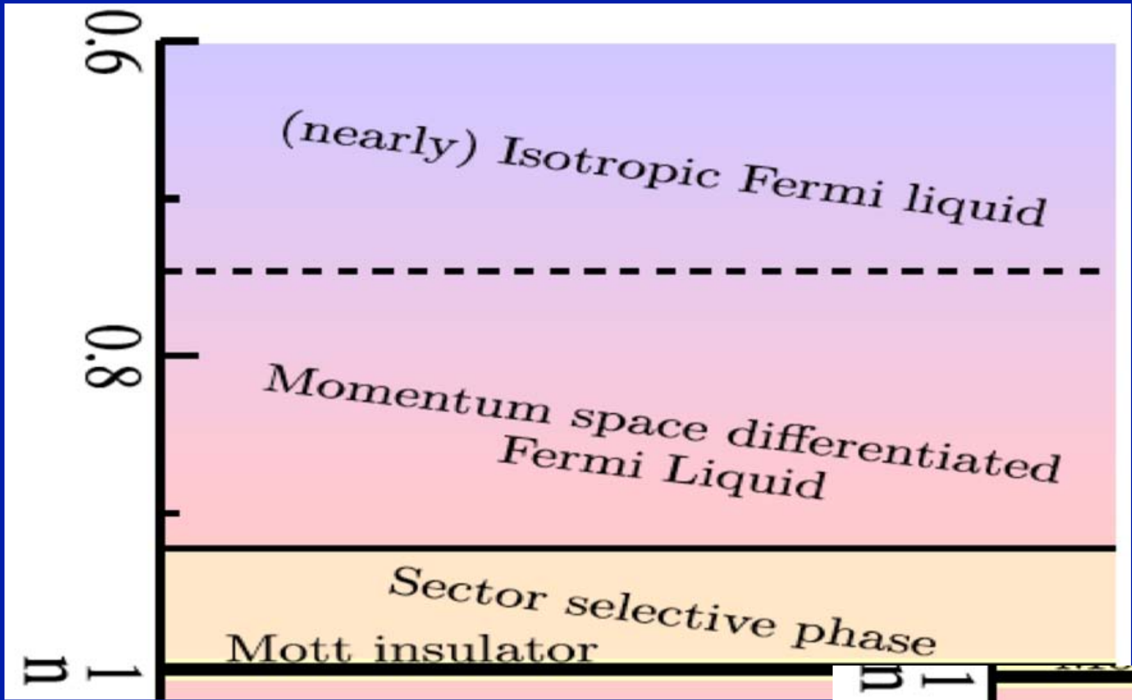

Hole doped

- Isotropic FL at hi-doping
- Momentum differentiation at intermediate doping
- Small HOLE-doping (only): <u>Momentum-sector selective Mott transition</u>

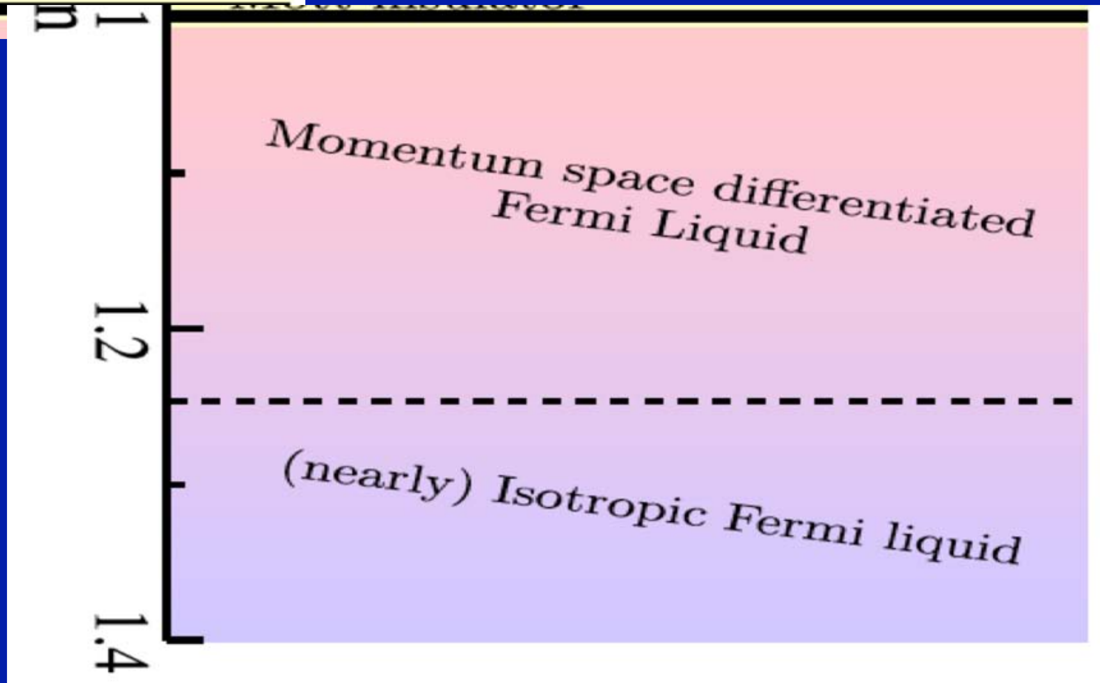

Electron doped

Momentum sector occupancy vs chemical potential: incompressibility of antinodes in sector-selective regime

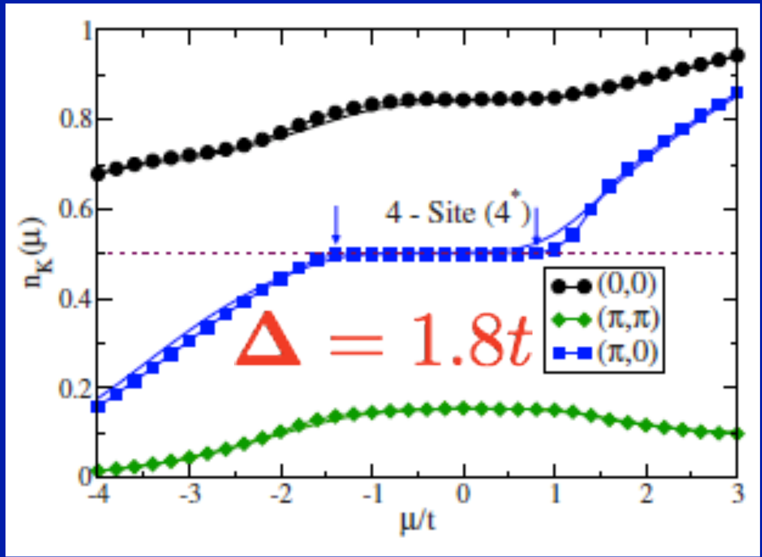

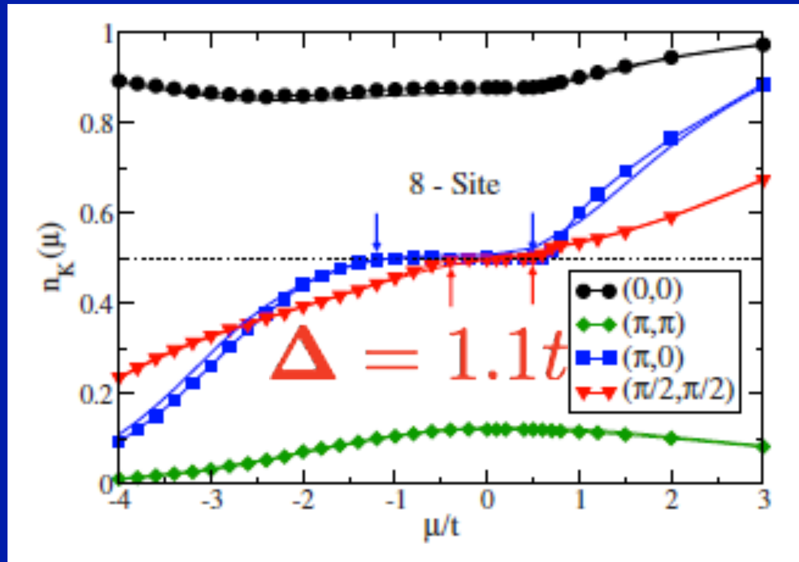

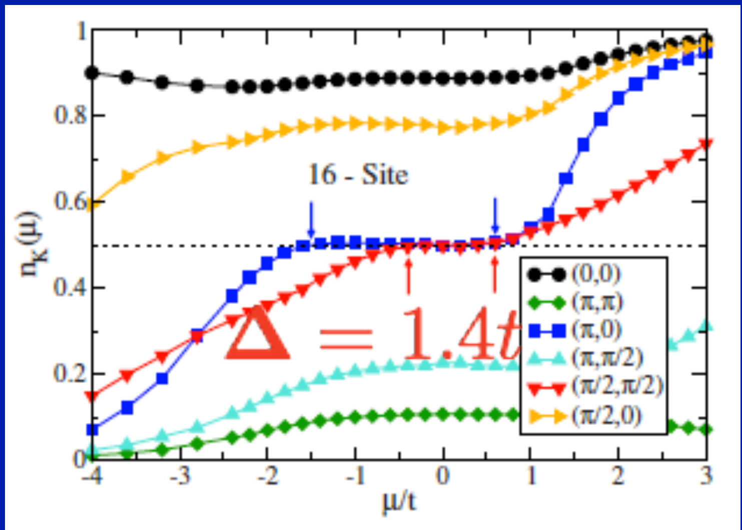

Cluster size	n^h_{diff}	n^e_{diff}	Δ_g	n^h_{SST}	Δ_{SST}
2	0.66	1.27	1.4		
4	0.65	1.38	2.6		2.6
4*	0.69	1.39	1.8	0.96	2.4
8	0.72	1.23	1.1	0.93	1.9
16	0.65	1.35	1.4	0.91	2.1

2-patch (VB-DMFT) theory adopts a somewhat special route to momentum selective transition:

Band edge of outer patch d.o.s

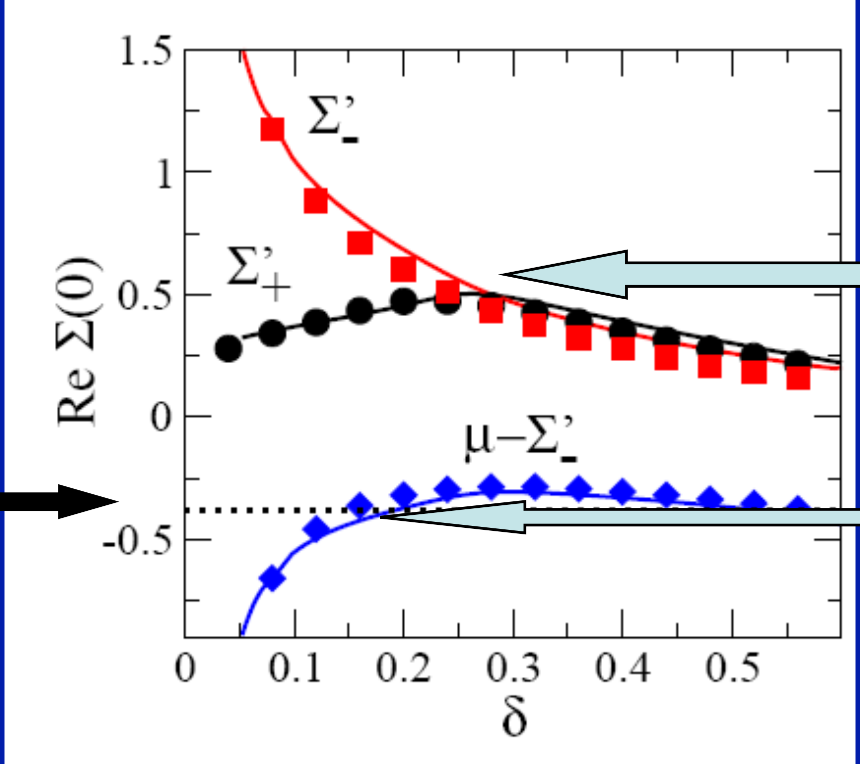

Onset of differentiation

Outer/odd Orbital gets (pseudo-) gapped

Zero-frequency self-energies vs. doping

- Low doping MS regime is dominated by formation of singlets on bonds (evolves to ~ Brinkman-Rice at higher doping)

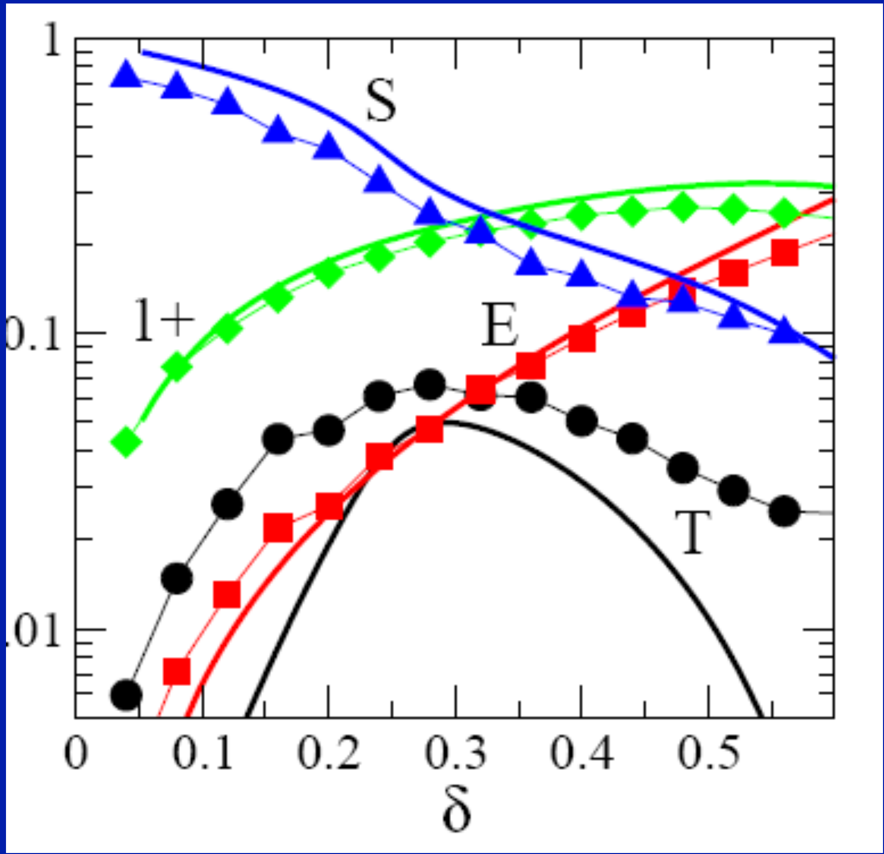

Statistical weights of the singlet (S) and 1-particle (1+) state vs. Doping in the CT-QMC calculation

Momentum-differentiated regime at intermediate doping level

A metal with anisotropic scattering rate

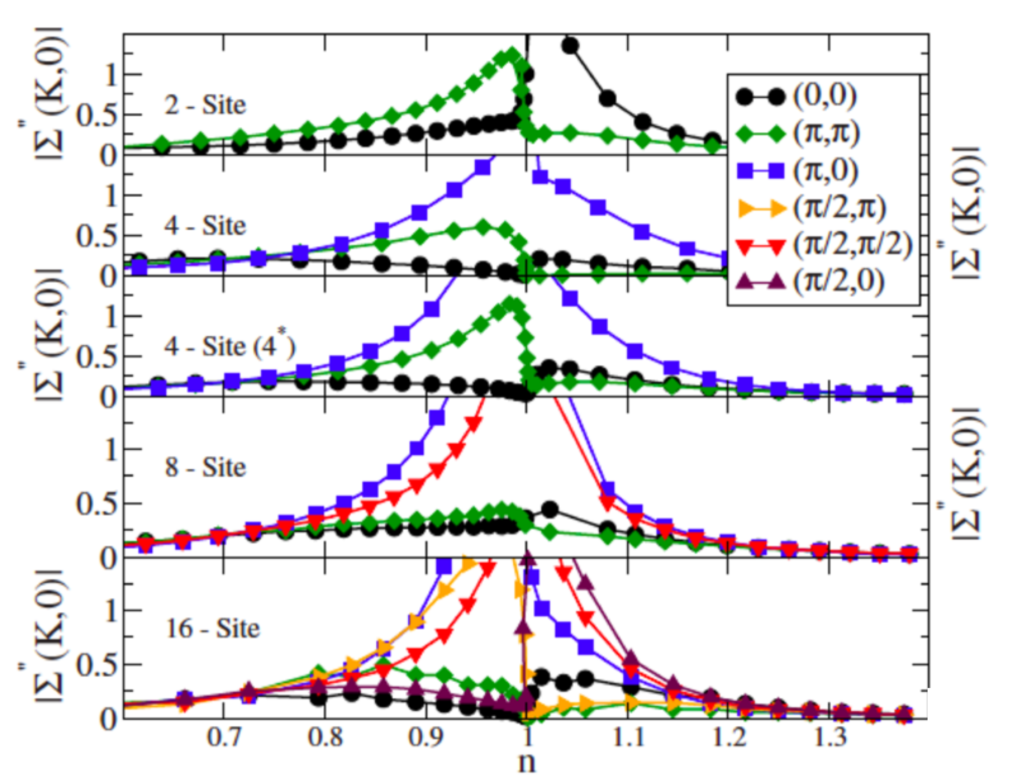

Antinodal scattering rate
Larger at small doping

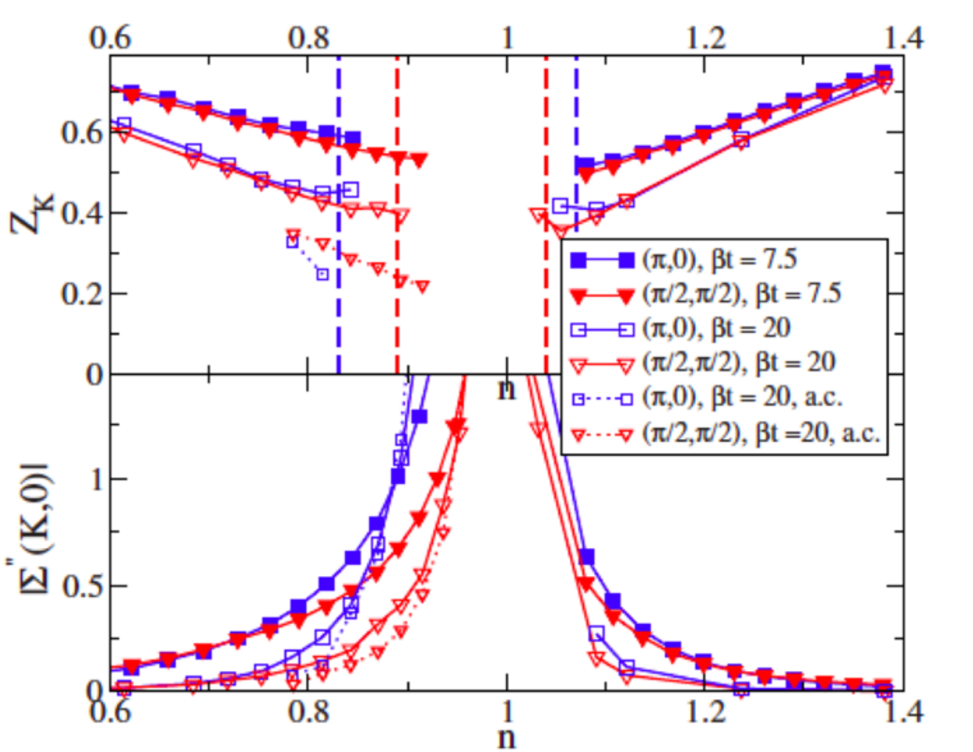

No clear Brinkman-Rice
Behavior of QP weights Z

T-dependence of scattering rate

$$\Sigma''(0)/T$$

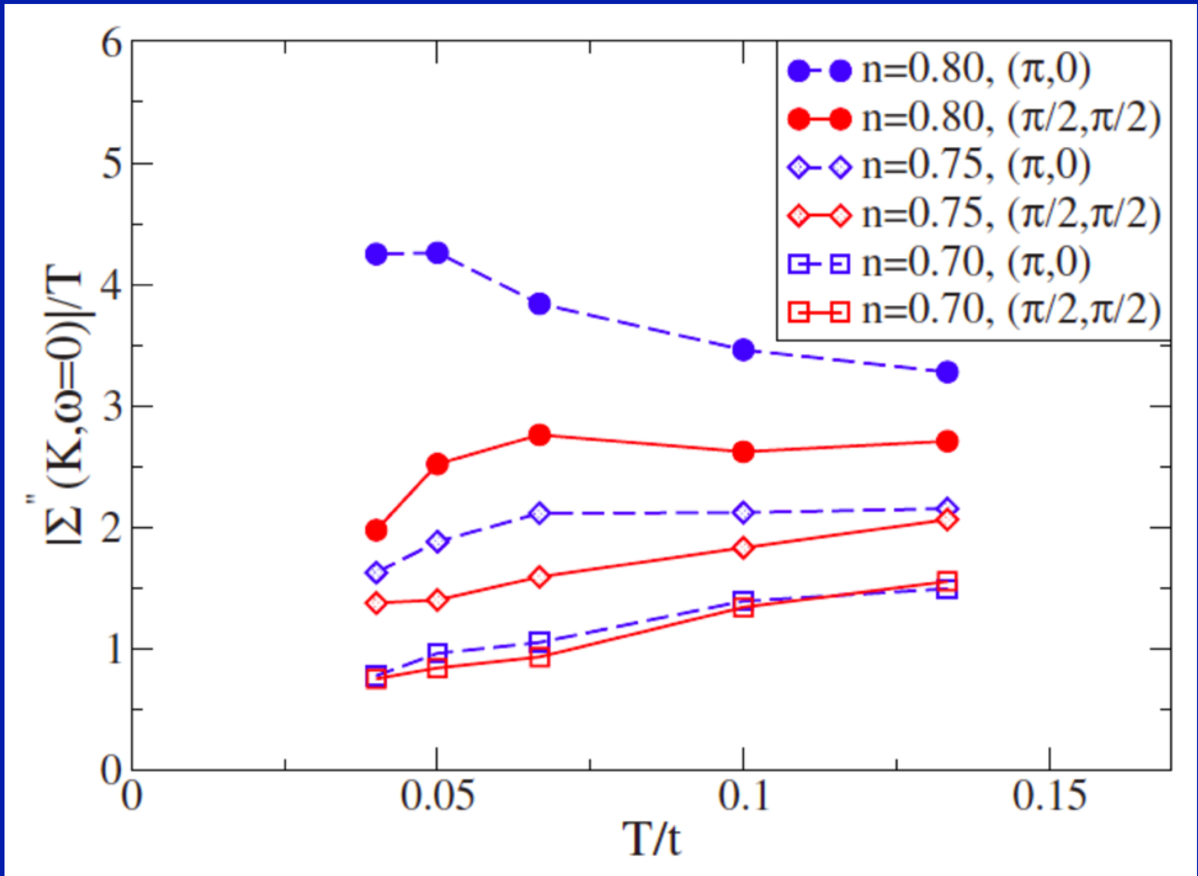

Nodal and Antinodal Behave differently at Small doping

Isotropic behavior at High doping

Qualitatively consistent with transport experiments: cf. N.Hussey J.Phys.CondMat (2008)

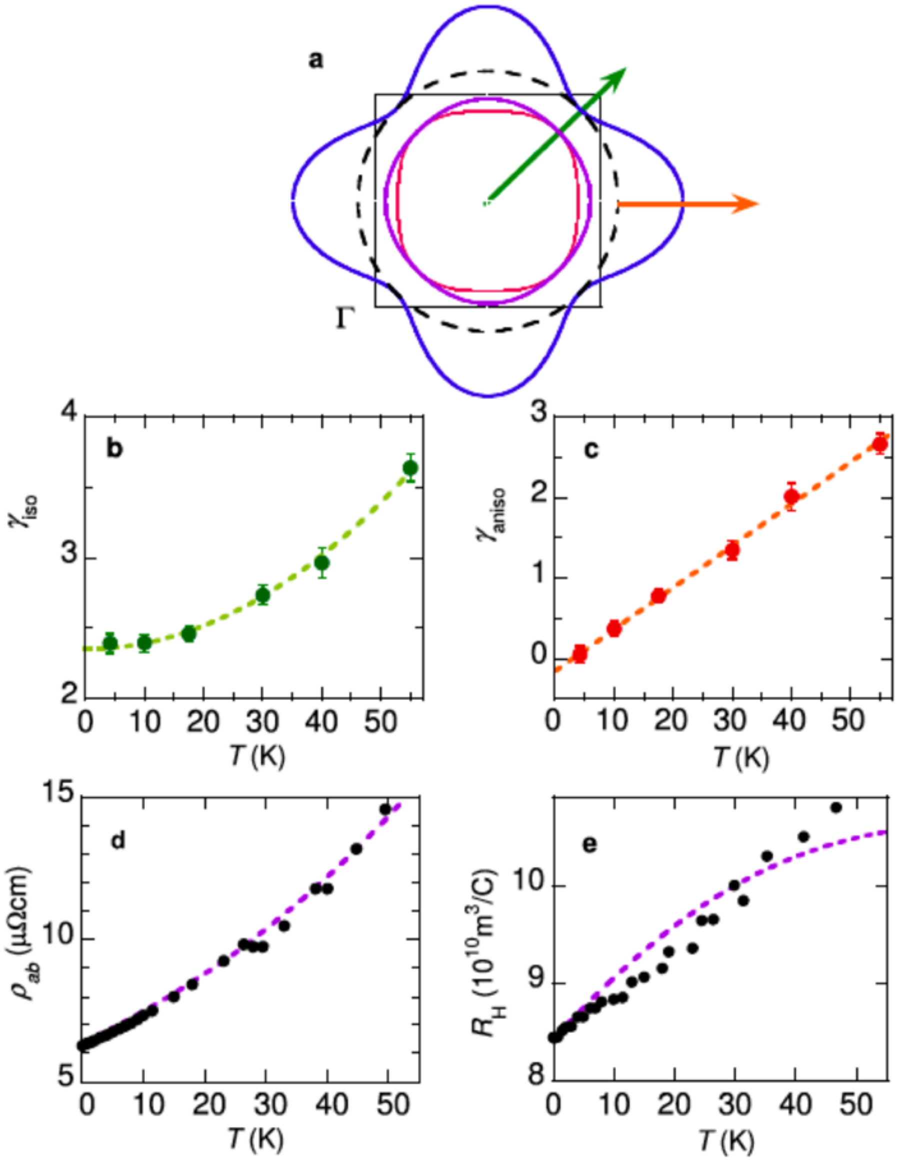

Figure 6. (a) Inner red curve: schematic 2D projection of the FS of overdoped Tl2201. Adjacent purple curve: schematic representation of the d-wave superconducting gap. Outer blue curve: geometry of $(\omega_c\tau)^{-1}(\varphi)$. Dashed black line: isotropic part of $(\omega_c\tau)^{-1}(\varphi)$. (b) T dependence of γ_{iso}, i.e. the isotropic component of $(\omega_c\tau)^{-1}(\varphi)$ and sole contribution along the 'nodal' region indicated by the green arrow in (a). The dashed curve is a fit to $A + BT^2$. (c) T dependence of γ_{aniso}, i.e. the anisotropic component of $(\omega_c\tau)^{-1}(\varphi)$ and the additional contribution that is maximal along the 'anti-nodal' direction indicated by the orange arrow in (a). The dashed curve is a fit to $C + DT$. (d) Circles: $\rho_{ab}(T)$ data for overdoped Tl2201 ($T_c = 15$ K) extracted from [49]. Dashed curve: simulation of $\rho_{ab}(T)$ from parameters extracted from the ADMR analysis. (e) Circles: $R_H(T)$ data for the same crystal [49]. Dashed curve: simulation of $R_H(T)$. Adapted with permission from *Nature Physics* 2 821, figure 2. Copyrig

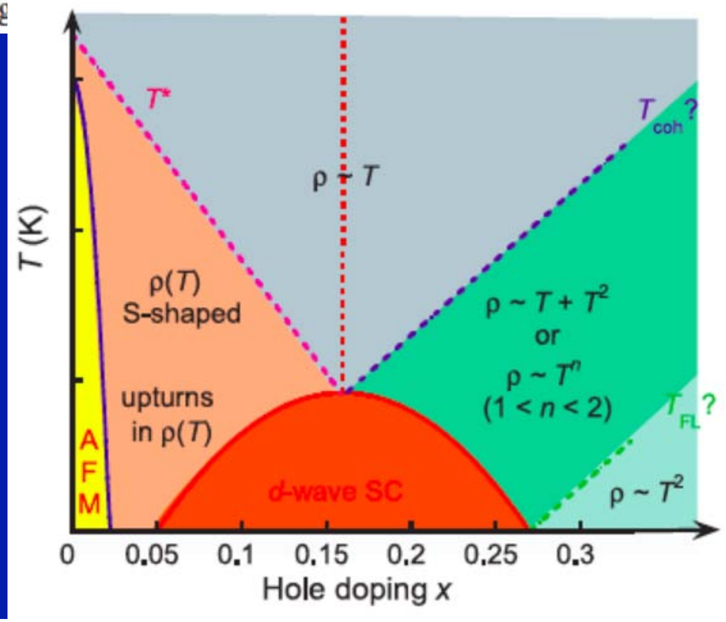

Pseudogap regime
(momentum sector-selective)

VB-DMFT/Antinode: not a sharp gap, a pseudogap!

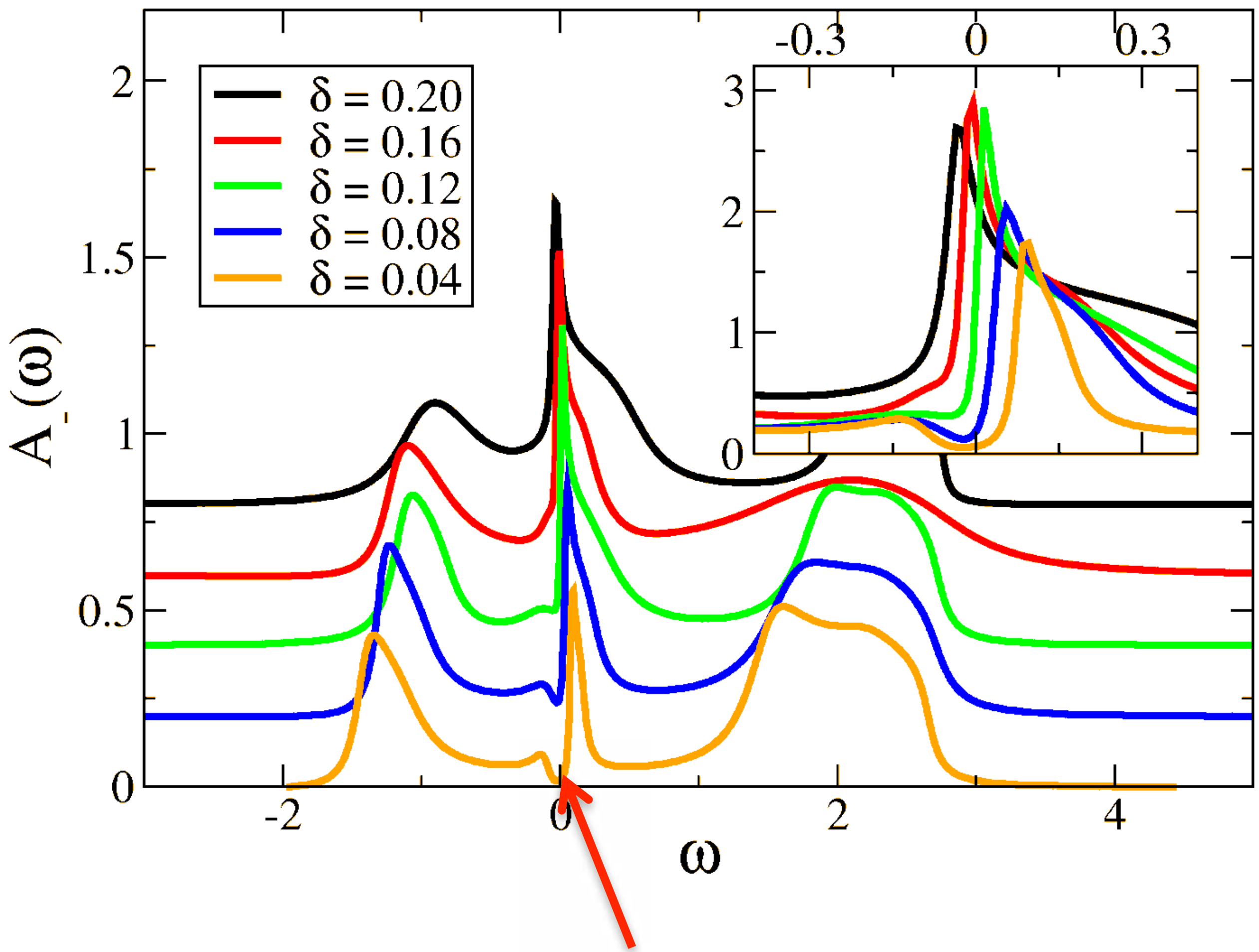

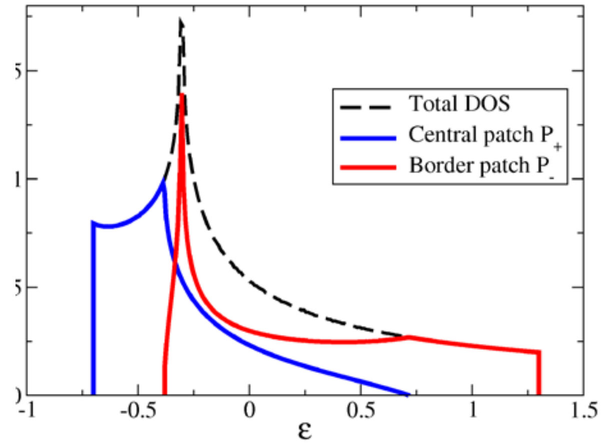

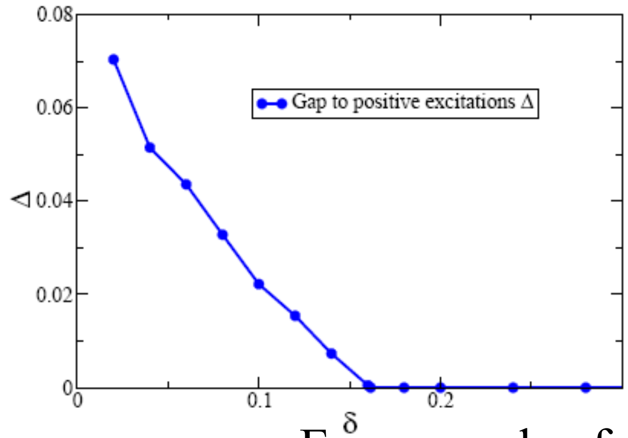

Energy scale of pseudogap on positive energy side

At the antinode, a pseudogap appears below the transition.

Correlations have a strong effect (e.g. prominent Hubbard bands)

Pseudogap opening upon cooling:

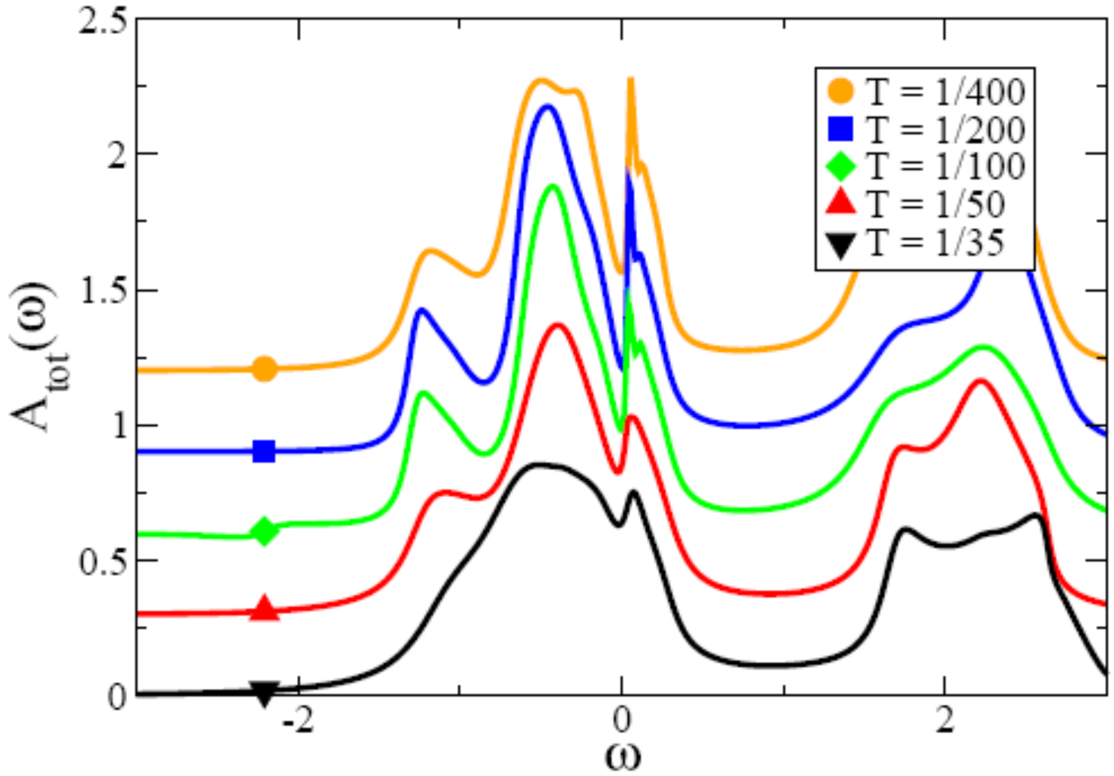

FIG. 10: (Color online) Total spectral function $A_{\rm tot}(\omega)$ for various temperature at $\delta = 0.08$. A shift of 0.3 has been added between each curves for clarity.

(Curves shifted upwards relative to one another, for clarity)

8-sites: pseudogap opening

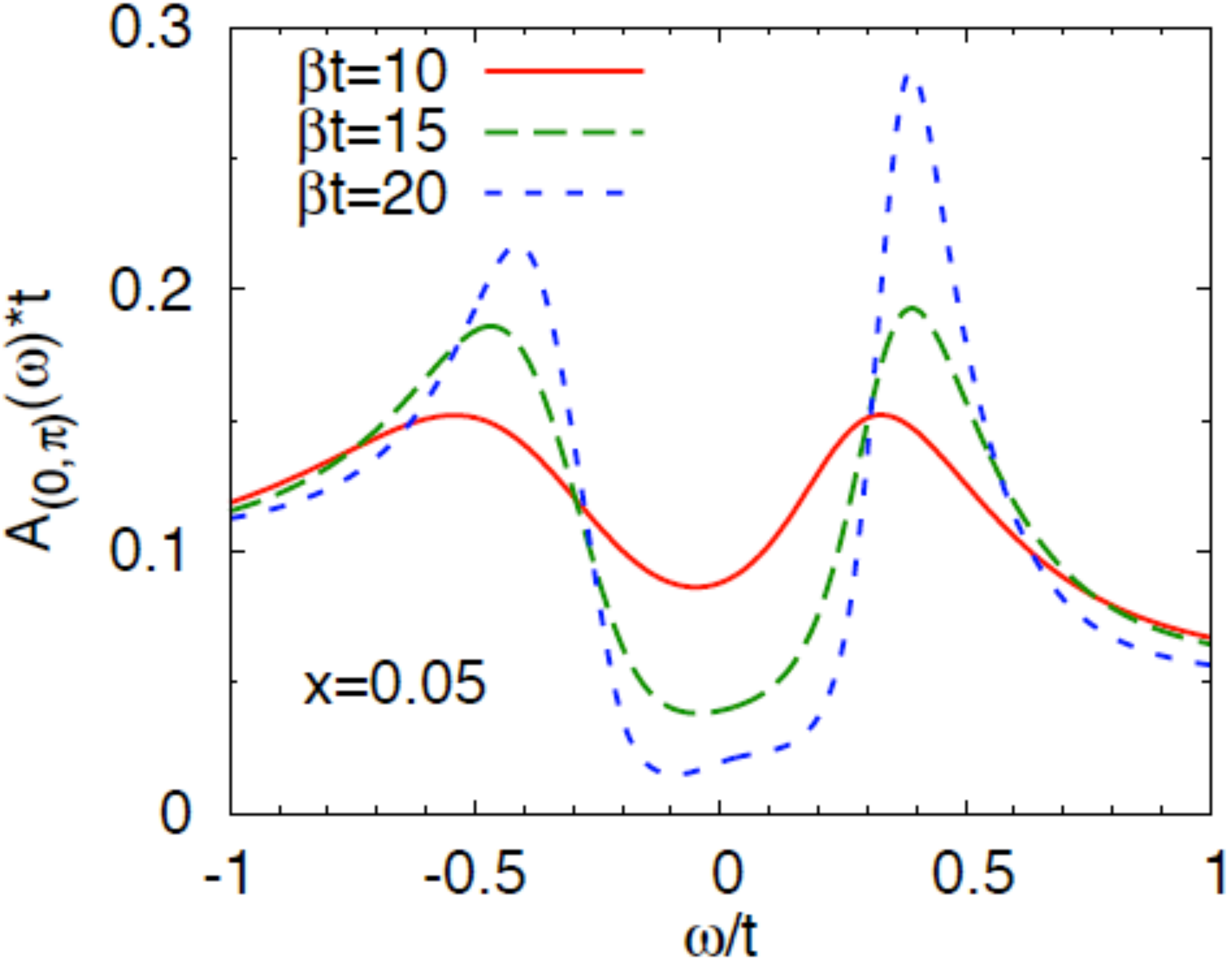

Werner, Gull, Parcollet, Millis, Lin

Calculated ARPES intensity maps

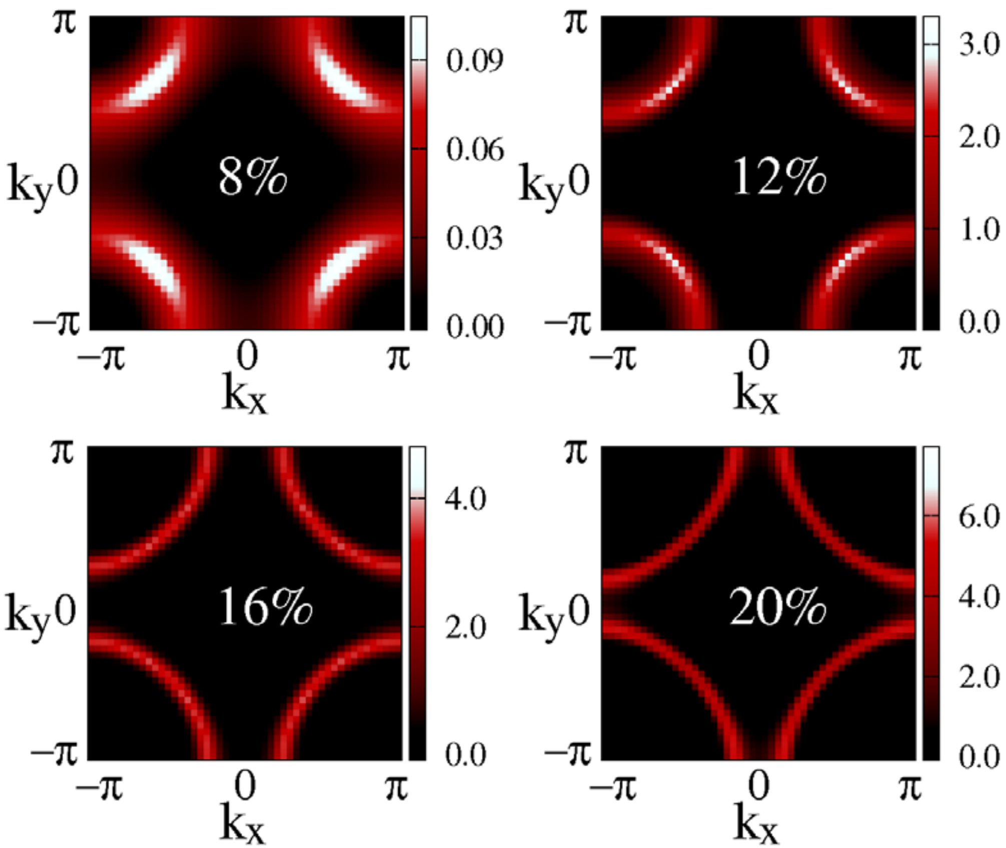

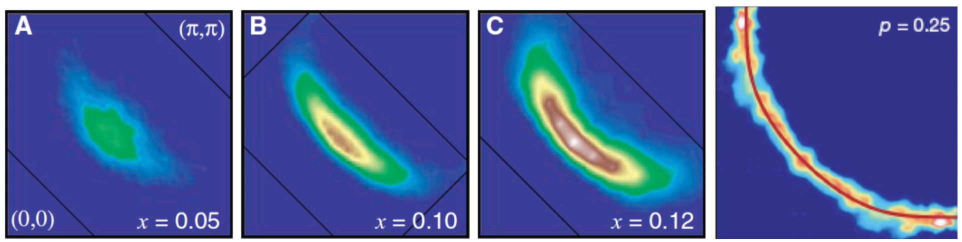

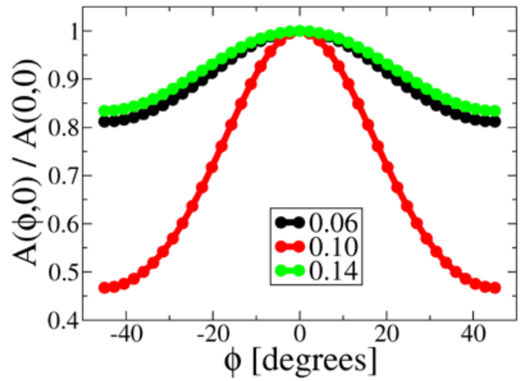

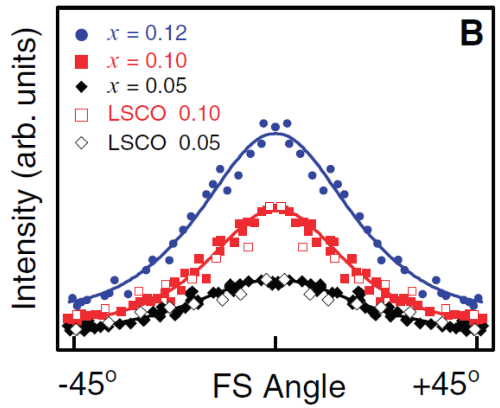

Shen et al., Science (2005)

Maximum contrast around 10%

With an (cumulant-) interpolation over the Brillouin zone…

Computed ARPES intensity maps

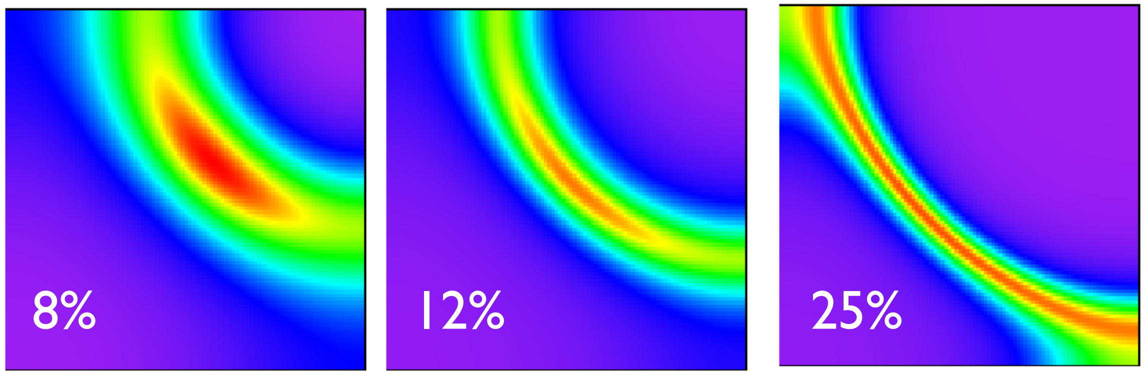

A(k,ω=0) contour map

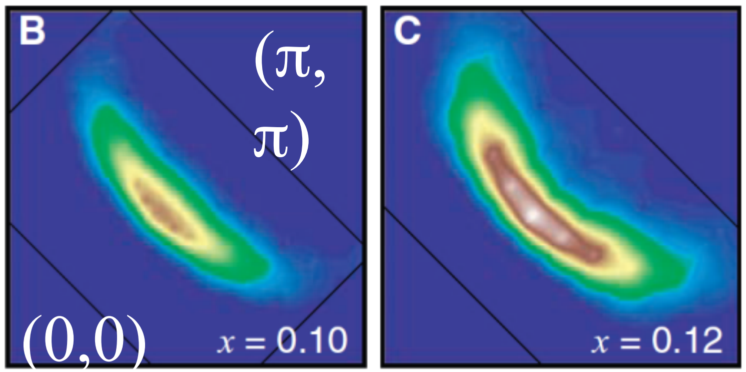

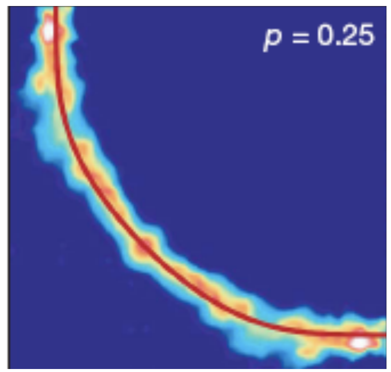

Shen et al., Science (2005)

Platé et al., PRL (2005)

With an interpolation over the Brillouin zone…

C-axis optical conductivity
M.Ferrero et al. PRB (2010)

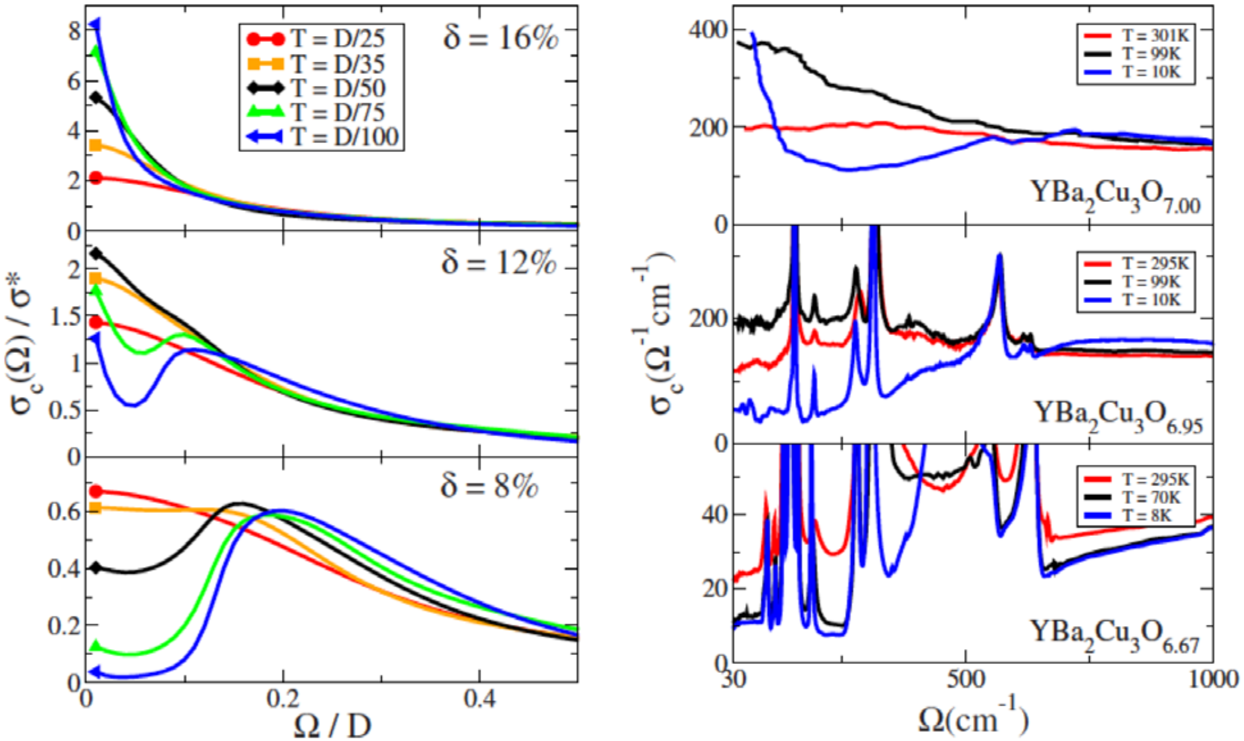

FIG. 2. (Color online) Left panel: the c-axis optical conductivity $\sigma_c(\Omega)$ calculated within VB-DMFT for three doping levels. σ_c is displayed in units of σ^* as defined in the text (σ^* is of order 50 Ω^{-1} cm^{-1} for $YBa_2Cu_3O_y$). Frequency is normalized to the half-bandwidth $D\sim 1$ eV=8000 cm^{-1}. Right panel: experimental data for the c-axis optical conductivity of $YBa_2Cu_3O_y$. The data for $YBa_2Cu_3O_{7.00}$ is taken from Ref. 8 where the phonon contribution was subtracted by fitting to five Lorentzian oscillators. The data for $YBa_2Cu_3O_{6.95}$ and $YBa_2Cu_3O_{6.67}$ are taken from Refs. 23 and 24.

$$\sigma_c(\Omega) = \frac{2e^2c}{\hbar ab}\int d\omega \frac{f(\omega)-f(\omega+\Omega)}{\Omega}\frac{1}{N}\sum_{\mathbf{k}} t_\perp^2(\mathbf{k})A(\mathbf{k},\omega)A(\mathbf{k},\Omega + \omega), \quad (2)$$

C-axis resistivity

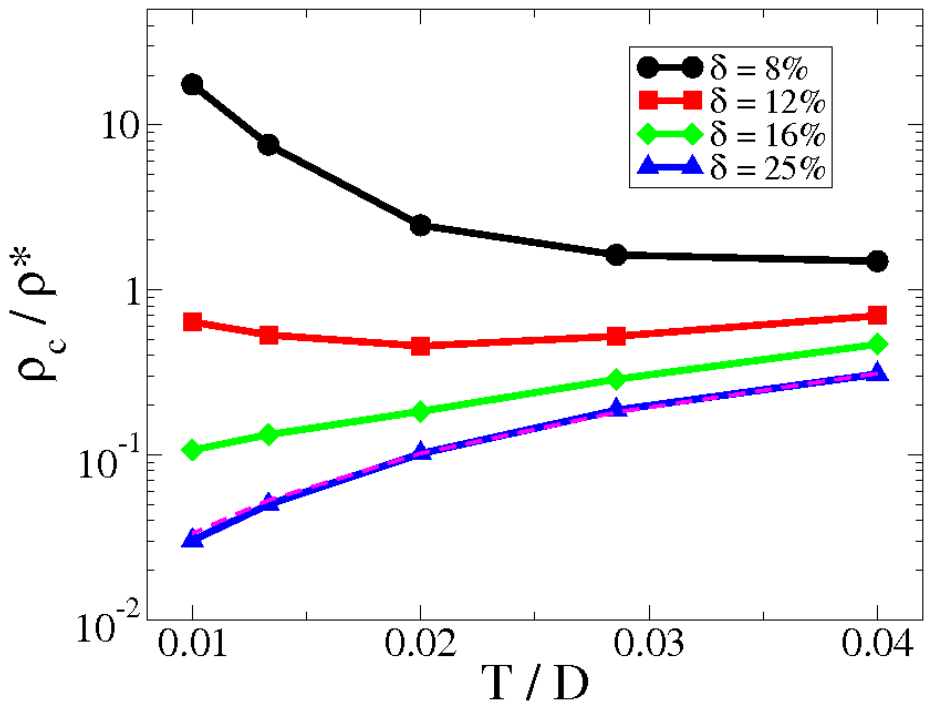

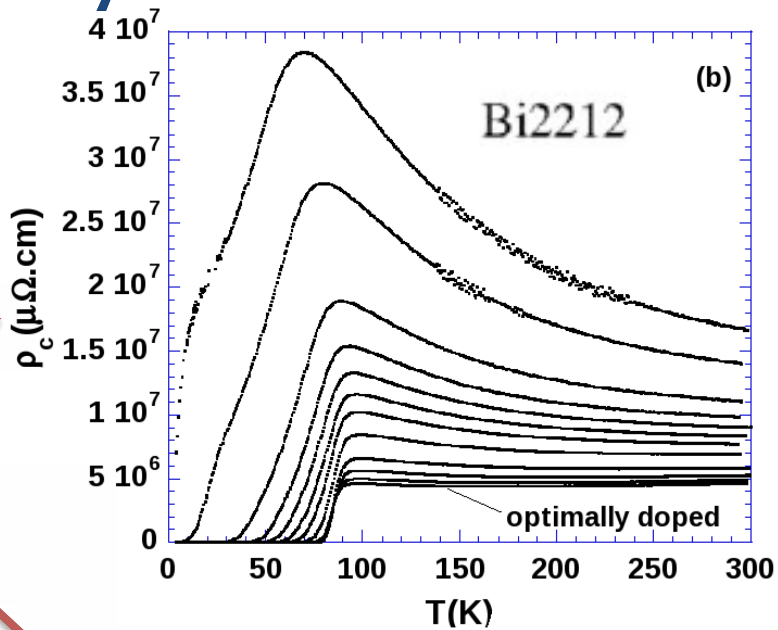

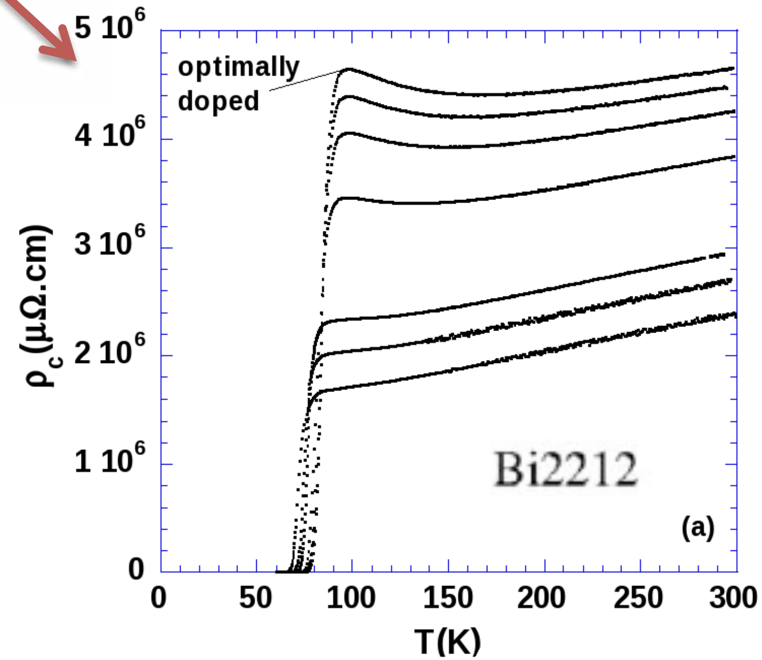

Overdoped: metallic
Underdoped: insulating
Optimally: minimum in resistivity

H. Raffy et al.

Take-home messages: cluster extensions of DMFT

- Proximity to Mott transition destroys antinodal quasiparticles
- Low-doping regime is dominated by the buildup of short-range singlet correlations (J), responsible for PG formation
- <u>Minimal</u> cluster-extension of DMFT accounts for nodal/antinodal differentiation
- PG appears as a momentum-sector selective Mott phase